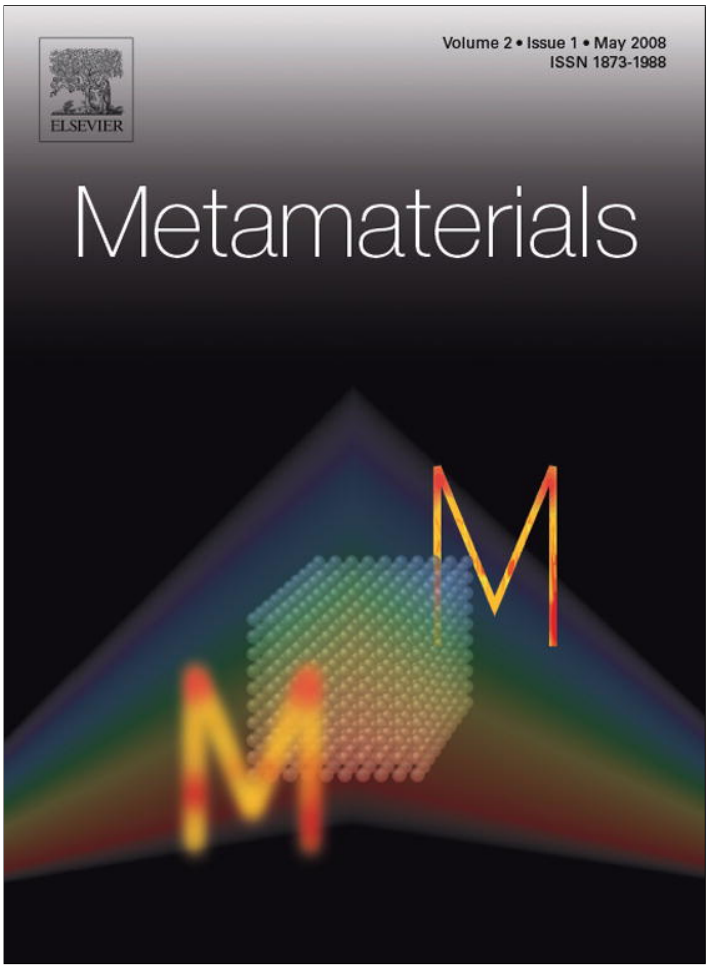

Available online at www.sciencedirect.com
ScienceDirect
Metamaterials 2 (2008) 1–17
Metamaterials
www.elsevier.com/locate/metmat

Invited Review

Fabrication of optical negative-index metamaterials: Recent advances and outlook

Alexandra Boltasseva [a,*], Vladimir M. Shalaev [b]

[a] *DTU Fotonik, Department of Photonics Engineering, Nano DTU, Technical University of Denmark, Oersdats Plads DTU-Building 343, DK-2800 Kongens Lyngby, Denmark*
[b] *School of Electrical and Computer Engineering & Birck Nanotechnology Center, Purdue University, West Lafayette, IN 47907, USA*

Received 20 December 2007; received in revised form 7 March 2008; accepted 12 March 2008
Available online 18 March 2008

Abstract

A status report on optical negative-index-metamaterial fabrication is given. The advantages, drawbacks and challenges of different fabrication techniques including electron-beam lithography (EBL), focused-ion beam (FIB) milling, interference lithography (IL) and nanoimprint lithography (NIL) and direct laser writing are outlined. Since the possibility of creating a truly three-dimensional (3D) metamaterial is critical for real-life applications and the future of this research area, the recent developments on large-scale, multiple-functional-layer metamaterials are discussed in detail, and alternative methods for 3D fabrication of complex structures are mentioned. Throughout the report, main breakthroughs in fabrication of optical negative-index metamaterials are described, as well as challenges facing future manufacturing of optical metamaterials.

PACS: 81.07.-b; 81.16.-c; 81.16.Nd

Keywords: Negative-index metamaterials; Nanofabrication; Nanolithography; Interference lithography; Nanoimprint

Contents

* Corresponding author. Tel.: +45 4525 6352; fax: +45 4593 6581.
E-mail address: aeb@com.dtu.dk (A. Boltasseva).

1873-1988/$ – see front matter © 2008 Elsevier B.V. All rights reserved.
doi:10.1016/j.metmat.2008.03.004

1. Introduction

On the path to new prospects for manipulating light, artificially engineered materials – metamaterials – attract a great deal of attention. When rationally designed, metamaterials demonstrate unprecedented electromagnetic properties that are unattainable with naturally occurring materials; by changing the design of the unit cell or "meta-atom", the optical properties of the metamaterial can be tailored, e.g., the values of permeability, μ, and permittivity, ε, can be controlled.

One of the most prominent examples of the properties that cannot be observed in natural materials is a negative refractive index [1–5]. If both permeability and permittivity are simultaneously negative, the refractive index becomes negative. Metamaterials that have a negative index of refraction (negative-index metamaterials or NIMs) may lead to the development of novel devices ranging from optical antennas with superior properties and a perfect lens (superlens and hyperlens), capable of imaging objects with resolution much smaller than the wavelength of light, to ultra-compact optical circuits and special coatings that can make an object invisible. These applications are of particular interest if such materials could be engineered to work at optical wavelengths. Although Veselago pointed out [1] that the combination $\varepsilon < 0$ and $\mu < 0$ leads to a negative refractive index, $n < 0$, this idea remained quite unappreciated for many years partially because no naturally occurring NIMs were known in the optical range. While there are natural materials with $\varepsilon < 0$ (e.g., gold, silver and other metals) up to the visible frequencies, magnetic materials with $\mu < 0$ do not normally exist at optical frequencies. This is because the material property limitations of natural materials imposed by their unit cells—atoms and molecules. One can overcome this limitation by instead using artificially structured metamaterials where "meta-atoms" are designed to exhibit both electric and magnetic responses in an overlapping frequency range. Recent scientific progress in the field of NIMs can be found, for example, in review papers [5,6].

Today's boom in NIM-related research, inspired by Sir John Pendry's prediction of the NIM-based superlens in 2000 [7], comes from recent advances in nanofabrication techniques that allow different materials to be structured on the nanometer scale. In man-made NIMs for the optical range of frequencies sub-wavelength until cells are specifically designed and densely packed into an effective composite material to exhibit the negative effective refractive index.

A first step towards the realization of a material with a negative index of refraction was done by Pendry et al. who suggested to use split-ring resonators (SRRs) as meta-atoms to achieve a magnetic permeability different from one [8], which is a needed step for obtaining a negative index. Such magnetic structures were successfully realized in the microwave [9], THz [10–12] and near-infrared (IR) optical range, 100 THz [13] and 200 THz [14]. For achieving magnetic response in the visible range another design of paired metal strips was successfully used by the Purdue group to show first a magnetic response in the red part of the spectrum [15] and then across the whole visible range [16].

Combining the negative-permeability structures with the negative-permittivity material (for example, simple metal wires arranged in a cubic lattice) can result in a negative-index material. Such a metamaterial was straightforward to accomplish in the microwave region [9].

The approaches for moving to shorter wavelengths were initially based on concepts from the microwave regime (such as split-ring resonators) with scaled down unit cell sizes. The main idea was that the magnetic resonance frequency of the SRR is inversely proportional to its size. Using single SRRs, this approach works up to about 200 THz [14,17,18]. However, this scaling breaks down for higher frequencies for the single SRR case because, for wavelengths shorter than the 200 THz range, the metal starts to strongly deviate from an ideal conductor [18]. For an ideal metal with infinite carrier density, hence infinite plasma frequency, the carrier velocity and the kinetic energy are zero, even for finite current in a metal coil. For a real metal, velocity and kinetic energy become finite. For a small SRR, non-ideal metal behaviour leads to a modified scaling law where the frequency approaches a constant and becomes independent of the SRR size [18]. This scaling limit combined with

the fabrication difficulties of making nanometer-scale SRRs along with metal wires led to the development of alternative designs that are more suitable for the THz and optical regimes.

One suitable design for optical NIMs is based on pairs of metal rods (also called "cut-wires") or metal strips, separated by a dielectric spacer. Such structures can provide a magnetic resonance $\mu < 0$ originating from antiparallel currents in the strips. An electric resonance with $\varepsilon < 0$ can result from the excitation of parallel currents [19] in the same strips. However, normally it is difficult to get the $\varepsilon < 0$ and $\mu < 0$ regions to overlap so a different design was proposed, the so-called "fishnet" structure. This structure combines the magnetic coupled strips (providing $\mu < 0$) with continuous "electric" strips that provide $\varepsilon < 0$ in a broad spectral range. NIMs at optical wavelengths were successfully demonstrated by using coupled cut-wires and fishnet structures [19–24].

To create a metamaterial at optical wavelengths, one should deal with small periodicities (about 300 nm and less) and tiny feature sizes (about 30 nm) to ensure effective-medium-like behaviour. Thus, the fabrication of optical NIMs is challenging since we aim at high-precision, high-throughput, and low-cost manufacturing processes. Feature sizes for metamaterials operating in the infrared or visible range can be smaller than the resolution of state-of-the-art photolithography (due to the diffraction limit), thus requiring nanofabrication processes with 100- or sub-100-nm resolution. Due to the limitations of current nanolithography tools, fabricated metamaterials do not really enter the real meta-regime where the unit cell size is orders of magnitude smaller than the wavelength. However, the feature size is typically small enough compared to the wavelength so that one can describe such material, at least approximately, as a medium with effective permeability, μ and permittivity, ε (which is in contrast to photonic crystals where the lattice period matches the wavelength).

In addition to sub-wavelength resolution, careful material choice is required for NIM fabrication. The choice of the metal for NIMs is crucial in the optical regime because the overall losses are dominated by losses in the metal components. Thus, their lowest losses at optical frequencies make silver and gold the first-choice metals for NIMs. Since the refractive index is a complex number $n = n' + in''$, where the imaginary part n'' characterizes light extinction (losses), a convenient measure for optical performance of a NIM is the figure of merit (FOM), defined as the ratio of the real and imaginary parts of n: $F = |n'|/n''$ (see, for example, [5,25]). Aside from the proper metal choice, loss compensation by introducing optically amplifying materials can be considered for achieving low-loss NIMs [26,27,28].

To make use of the novel optical properties of metamaterials, where meta-atoms are designed to efficiently interact with both the electric and magnetic components of light, one has to create a slab of such a material with an interaction length of many light wavelengths. Together with the novel fundamental properties of NIMs, entirely new regimes of nonlinear interactions were predicted for such materials (see, for example, [27–37]). For all exciting applications to be within reach, the next issue to address (in addition to losses) is the development of truly three-dimensional (3D) NIMs in the optical range. The challenging tasks here are to move from planar structures to a 3D slab of layered metamaterial and to develop new isotropic designs.

With the development of low-loss large-scale optical NIMs, many new device concepts will emerge empowered by optical magnetism and new regimes of linear and nonlinear light-matter interactions. Materials to manipulate an object's degree of visibility, sub-wavelength imaging systems for sensors and nanolithography tools, and ultra-compact waveguides and resonators for nanophotonics are only a few examples of possible metamaterial applications. For example, among the most exciting new applications for 3D low-loss metamaterials are those based on transformation optics [38–40], including hyperlenses that enable sub-wavelength far-field resolution [41–46] and designs for optical cloaking [38,47–49].

In this paper, we review the recent progress in fabrication of metal–dielectric nanostructured metamaterials at optical wavelengths, and outline alternative manufacturing techniques that can be adapted for future NIM fabrication.

2. First experimental demonstrations: single metamaterial layer

Proof-of-principle studies of optical NIMs were performed on two-dimensional (2D) structures—a single layer of a metamaterial created on top of a transparent substrate. The first experimental demonstrations of negative refractive index in the optical range were accomplished nearly at the same time for two different metal–dielectric geometries: pairs of metal rods separated by a dielectric layer [19] and the inverted system of pair of dielectric voids in a metal–dielectric–metal multiplayer [20] (Fig. 1).

In the first example, an array of pairs of parallel 50-nm-thick gold rods separated by 50 nm of SiO_2 spacer was fabricated using electron-beam lithography (EBL)

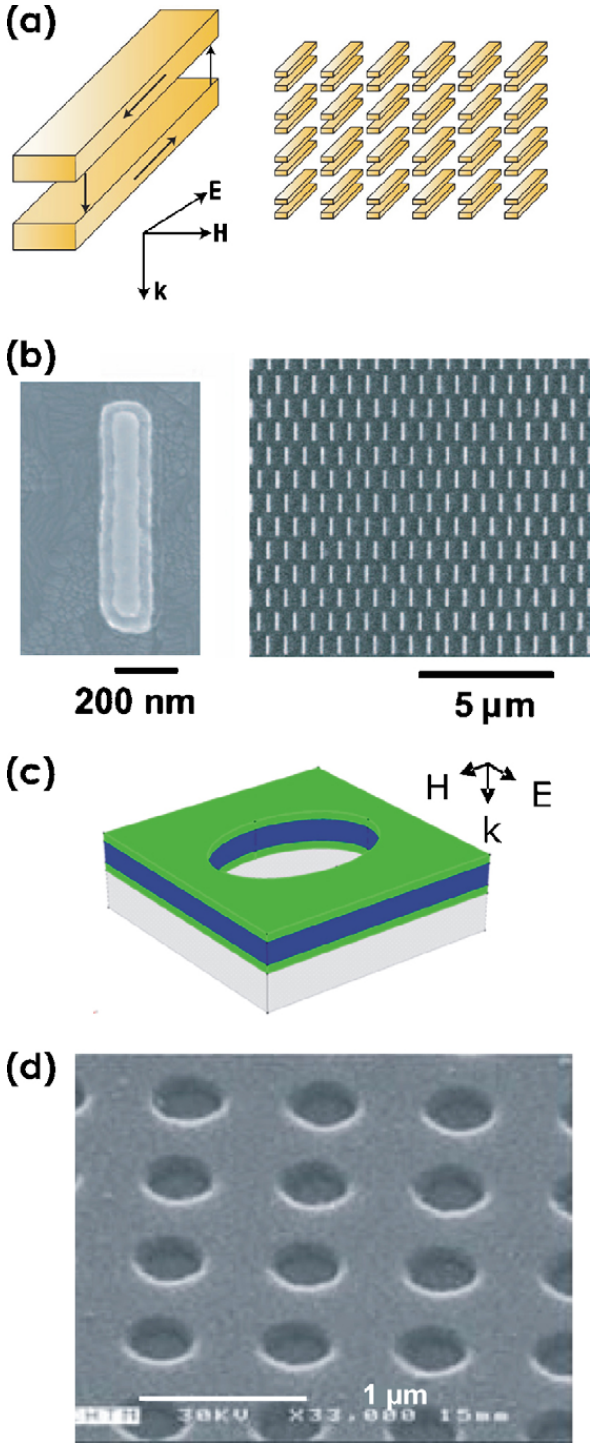

Fig. 1. First experimentally obtained optical negative-index metamaterials: (a) schematic of an array of paired Au nanorods separated by a layer of SiO_2 together with (b) field-emission scanning electron microscope images of the fabricated array (Au(50 nm)–SiO_2(50 nm)–Au(50 nm) stacks), where a negative refractive index is achieved at telecommunication wavelengths [19]; (c) schematic of a multilayer structure consisting of a dielectric layer between two metal films perforated with a hole on a glass substrate; (d) scanning electron microscope image of the fabricated structure (Au(30 nm)–Al_2O_3(60 nm)–Au(30 nm) stack, 838 nm pitch, 360 nm hole diameter), which exhibits a negative index at about $\lambda \approx 2$ μm [20].

via a standard lithography – deposition – lift-off process [15,19,22,24]. The coupled rods-based NIM exhibited a negative refractive index of $n' \approx -0.3$ at 1.5 μm [19]. In the other work, interference lithography (IL) with a 355-nm UV source was used to define a 2D array of holes in a multilayer structure (60-nm-thick Al_2O_3 dielectric layer between two 30-nm-thick Au layers), and the structure was shown to exhibit a negative refractive index of -2 around 2 μm [20]. Being the first proof-of-principle experiments, these structures had a high-loss coefficient (so that the FOM was small).

3. Fabrication of 2D metamaterials

3.1. Standard method: electron-beam lithography

Due to the fact that the required feature sizes for optical NIM fabrication are smaller than the resolution of state-of-the-art photolithography, 2D metamaterial layers are normally fabricated using electron-beam lithography [19,21,22]. In EBL, a beam of electrons is used to generate patterns on a surface. Beam widths can be on the order of nanometers, which gives rise to the high nanoscale resolution of the technique. EBL is a serial process wherein the electron beam must be scanned across the surface to be patterned. The EBL technique is quite versatile at the point of initial design and preliminary studies of optical properties of metamaterials since it offers sub-wavelength resolution and almost complete pattern flexibility. In the past 2 years, different NIM structures were successfully fabricated by EBL and experimentally investigated by several groups. When compared to the first structures [19,20], second-generation NIMs showed improved optical performance via higher figures of merit (i.e., lower losses).

The best-performance (the largest figure of merit) negative-refractive-index material at the telecommunication wavelength was achieved by the Karlsruhe group in collaboration with Iowa State University in 2006 [22]. The results were obtained for a fishnet structure [25], which could be viewed as an array of rectangular dielectric voids in parallel metal films (rather than circular voids as in Ref. [20]). A refractive index in the fabricated fishnet structure (lattice constant 600 nm) based on a sandwich of Ag(45 nm)–MgF_2(30 nm)–Ag(45 nm) was reported to reach $n' = -2$ at $\lambda \approx 1.45$ μm.

Moving to shorter wavelengths, two groups recently reported negative refractive index results in the visible range: the Karlsruhe group ($n' = -0.6$ at 780 nm) [23] and a group at Purdue University ($n' = -0.9$ and -1.1 at about 770 nm and 810 nm, respectively) [24] (Fig. 2). We

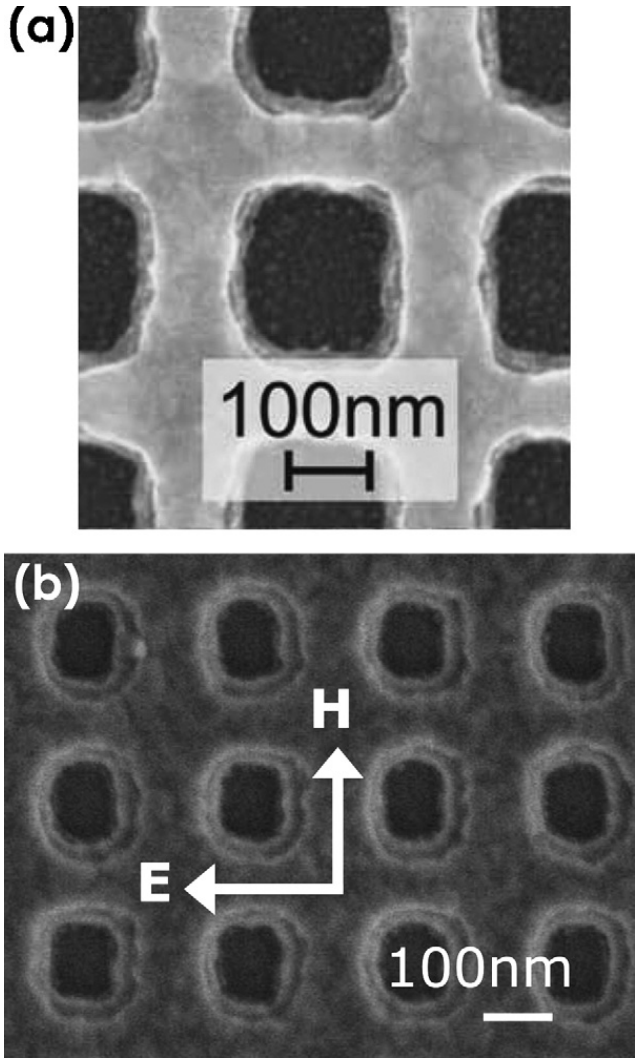

Fig. 2. Scanning electron microscope images of nano-fishnets fabricated by electron-beam lithography, metal–dielectric–metal stack deposition and a lift-off procedure: (a) by the Karlsruhe group ($n' = -0.6$ at 780 nm, Ag(40 nm)–MgF_2(17 nm)–Ag(40 nm) stack, lattice constant 300 nm) [23] and (b) by the Purdue group ($n' = -0.9$ at 772 nm, Ag(33 nm)–Al_2O_3(38 nm)–Ag(33 nm), lattice constant 300 nm) [24]. The smallest feature is below 100 nm, sidewalls are quite rough [23].

note while the demonstrated NIMs at 780 nm and 770 nm were single negative (i.e., even thought $n < 0$ was accomplished, μ remained positive at these wavelengths), the Purdue material at 810 nm was double-negative, with both ε and μ simultaneously negative at 810 nm, resulting in a larger (exceeding one) figure of merit. Both designs were based on nano-fishnets made in either Ag–MgF_2–Ag [23] or Ag–Al_2O_3–Ag [24] multilayer structures with the smallest features below 100 nm. The fabricated structures had good large-scale homogeneity. However, due to sub-100-nm features required for visible-range NIMs (68 nm minimum in-plane feature size at 97 nm thickness of the Ag–MgF_2–Ag sandwich [23]), the aspect ratio (height/width) for these NIM stacks can exceed unity. This gives rise to significant fabrication challenges connected to the lift-off procedure, and to increased sidewall roughness [23] (Fig. 2).

Even though EBL is normally used to write relatively small areas, large-area all-dielectric planar chiral metamaterials were recently fabricated by EBL [50,51]. In this approach, the use of a charge dispersion layer solves stitching errors during the serial writing process, which enables the fabrication of good-quality structures without the limitations normally encountered by stitching errors and field alignment.

The fabrication of optical NIMs is quite challenging due to the fabrication requirements of small periodicities (near and below 300 nm) and tiny feature sizes (down to several tens of nm). Thus, EBL is still the method of choice for fabricating metamaterials despite low throughput of the serial point-by-point writing and high fabrication costs. Since only small areas (of the order of 100 μm × 100 μm) can normally be structured within reasonable time and at reasonable costs, EBL does not offer a solution for the large-scale NIM fabrication required by applications, where many square centimeters have to be nanopatterned.

3.2. *Rapid prototyping: focused-ion beam (FIB) milling*

For rapid prototyping of metamaterials, focused-ion beam milling techniques can be used. In FIB, a focused beam of gallium ions is used to sputter atoms from the surface or to implant gallium atoms into the top few nanometers of the surface, making the surface amorphous. Because of the sputtering capability, the FIB is used as a micro-machining tool, to modify or machine materials at the micro- and nanoscale. Recently, this technique was used for fabricating magnetic metamaterials based on split-ring resonators [17]. Scaling of the SRR structure requires sub-100-nm gap sizes (down to 35 nm) for a 1.5 μm resonance wavelength, thus requiring state-of-the-art nanofabrication tools. For such small features, EBL-based fabrication requires time-consuming tests and careful optimization of writing parameters and processing steps, leading to relatively long overall fabrication times. In contrast, the rapid prototyping of complete structures can be fabricated via FIB writing in times as short as 20 min [17]. The process is based on FIB writing and corresponds to an inverse process where the FIB removes metal (20 nm of Au) deposited on a glass substrate. After FIB writing the structure is ready and no further post-processing steps are required.

Focused-ion beam nanofabrication might be of preference for fabricating specific (e.g., SRR-based) designs of metamaterials as in the above example. However, for creating an optical NIM, SRRs have to be combined with other metallic structures that can provide negative permittivity [5]. This will give rise to additional processing steps and delicate considerations regarding the choice of process parameters and materials. Moreover, moving SRRs from the telecom to the visible range will bring the process to the limit of size scaling in SRRs [18]. Thus, due to design and material limitations combined with low throughput, FIB has certain limitation in its use for fabricating optical NIMs. However, it should be mentioned that for some specific designs and proof-of-principle experiments, for example including nonlinear materials, FIB is the first choice for rapid prototyping.

3.3. *Large-scale fabrication: interference lithography*

The only large-scale manufacturing technique used so far by the integrated circuit industry is optical lithography (OL). Nowadays, OL continues to be extended and offers new ways of increasing its resolution, for example, by using immersion techniques that meet the industry needs for 45-nm half-pitch nodes [52]. One type of OL, namely interference lithography, is a powerful technique for the fabrication of a wide array of samples for nanotechnology. This fabrication technique is based on the superposition of two or more coherent optical beams forming a standing wave pattern. Being a parallel process, IL provides a low-cost, large-area (up to $\sim$cm^2) mass-production capability. Moreover, multiple exposures, multiple beams, and mix-and-match synthesis with other lithographic techniques can extend the range of IL applicability [52]. IL offers high structural uniformity combined with considerable, but not total, pattern flexibility while its resolution is now approaching the 20-nm scale [52].

Since NIM fabrication requires a periodic or quasi-periodic pattern, IL is an excellent candidate for large-area metamaterial fabrication. Recently, interference lithography was employed for the fabrication of one-dimensional metallic structures [53], magnetic metamaterials at 5 μm and 1.2 μm wavelength [11,53], and, as mentioned above, NIMs at 2 μm [20,54] (Fig. 1). Using this technique, the fabrication of square-centimeter-area structures was demonstrated [11,53,54] as well as the large-area homogeneity [53]. For example, a large-scale NIM created by making elliptical voids in an Au(30 nm)–Al_2O_3(75 nm)–Au(30 nm) multilayer stack was found to exhibit $n' \approx -4$ at 1.8 μm (Fig. 3)

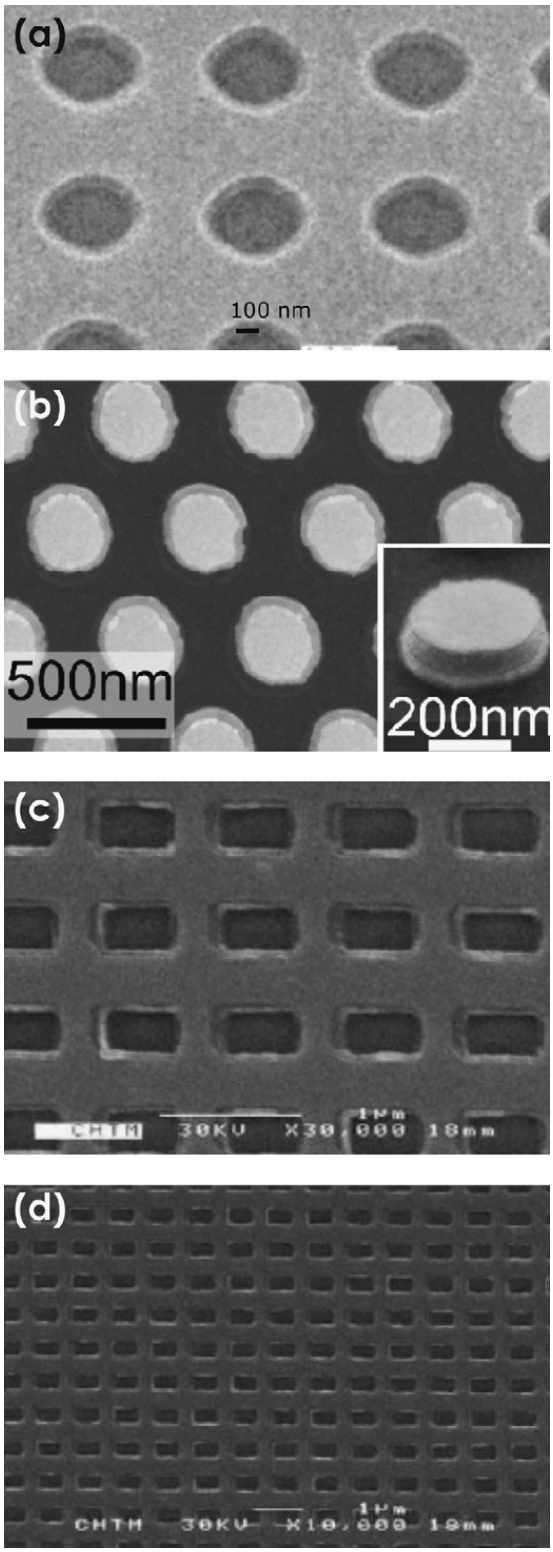

Fig. 3. Scanning electron microscope images of samples made by interference lithography: (a) a NIM based on coupled voids in a Au(30 nm)–Al_2O_3(75 nm)–Au(30 nm) multilayer structure (pitch 787 nm, hole sizes 470 nm and 420 nm) [55] and (b) a hexagonal 2D structure built by Au(20 nm)–MgF_2(60 nm)–Au(20 nm) pillars on a glass substrate [53], (c and d) fishnet structure samples in a Au(30 nm)–Al_2O_3(60 nm)–Au(30 nm) multilayer structure (528 nm, 339 nm on long and short sides, respectively) [56].

[55]. Very recently, for three different IL-fabricated NIM structures, a negative refractive index was obtained over a range of wavelengths: 1.56–2 μm, 1.64–2.2 μm and 1.64–1.98 μm for NIMs with circles, ellipses and rectangles (fishnet), respectively (Fig. 3) [56].

The results mentioned above established IL as a new direction for the design and fabrication of 2D optical NIMs and highlighted the advantages of such a large-area patterning technique. The technique is compact, robust, does not require expensive cleanroom equipment and can provide sample areas up to many square centimeters by up-scaling the apertures of the optics [53].

Given the simplicity and robustness of making a high-quality, single layer of a metamaterial using IL, one can envision further investigations aiming at piling 2D layers to create a 3D structure. Such a transition to 3D fabrication will turn parallel IL process into a step-by-step procedure that would require alignment of subsequent layers. Even though for compact versions of IL such a transition might result in a time-consuming fabrication process due to multiple alignments, proper technique development would make it possible to optimize and automate the alignment procedure. Thus, IL can be considered to be one approach for making 3D optical NIMs.

3.4. High-resolution large-scale fabrication: nanoimprint lithography (NIL)

Another promising direction for the fabrication of production-compatible, large-area, high-quality optical NIMs at low processing cost and time is offered by nanoimprint lithography [57]. A next generation lithography candidate, NIL accomplishes pattern transfer by the mechanical deformation of the resist via a stamp rather than a photo- or electro-induced reaction in the resist as in most lithographic methods. Thus the resolution of the technique is not limited by the wavelength of the light source, and the smallest attainable features are given solely by stamp fabrication. Moreover, NIL provides parallel processing with high throughput. Since NIM fabrication requires high patterning resolution, NIL is well suited for large-scale production of optical NIMs, providing wafer-scale processing using standard cleanroom procedures combined with simplicity and low cost.

Lately, two types of NIMs operating at near- and mid-IR frequencies, respectively, were fabricated via NIL. The first structure comprised ordered "fishnet" arrays of metal–dielectric–metal stacks that demonstrated negative permittivity and permeability in the same frequency region and hence exhibited a negative refractive index of $n' \approx -1.6$ at a wavelength near 1.7 μm [58] (Fig. 4). In the mid-IR range, the metamaterial was an ordered

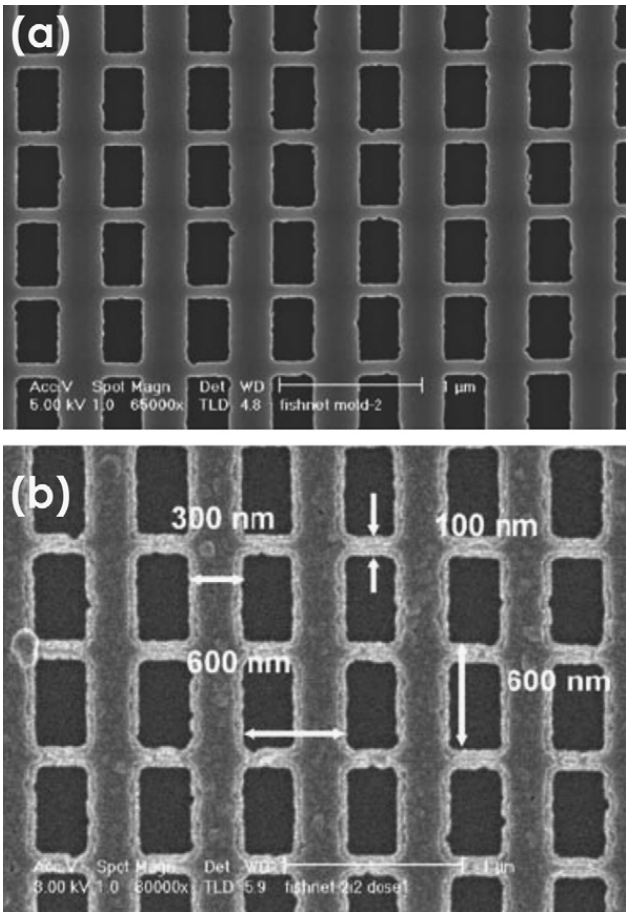

Fig. 4. SEM images of the (a) NIL mould and (b) fabricated fishnet pattern (Ag(25 nm)–SiO_x(35 nm)–Ag(25 nm) NIM stack) [58].

array of fourfold symmetric L-shaped resonators (with a minimum feature size of 45 nm) that were shown to exhibit negative permittivity and a magnetic resonance with negative permeability near wavelengths of 3.7 μm and 5.25 μm, respectively [59]. The smallest achieved feature sizes were about 100 nm and 45 nm for near- and mid-IR NIMs, respectively. Earlier, room temperature NIL was successfully applied to the fabrication of planar, chiral, photonic metamaterials for the study and application of novel polarization effects where both dielectric and metallic metamaterials with feature sizes from micrometric scale down to sub-100 nm were fabricated [60].

Recently, the possibility of a more simplified NIL method for creating metallic 2D structures was also proposed [61]. The technique is based on direct, hot embossing into metals (for example, Al) using hard templates like SiC [62]. In this approach, metal nanostructures can be obtained by printing directly on metal substrates without any further processing step (when compared to standard lithography and etching/deposition steps), thus simplifying the processing

steps and lowering the production cost. Using these hard moulds, successful pattern transfer directly to Al substrates as well as Au films has been achieved by pressing at room temperature [62]. However, this method has some challenges in the technical development of this approach, mostly connected to the fabrication of the hard stamps. Moreover, for the existing NIM designs it cannot be directly applied to the fabrication of optical NIMs due to specific requirements on geometry and materials.

4. Fabrication of 3D metamaterials

4.1. Making multiple layers

Recently, a low-loss optical NIM with a thickness much larger than the free-space wavelength in the near-infrared region was numerically demonstrated [63]. In the work by Zhang et al., simulations showed that a NIM slab consisting of multiple layers of perforated metal–dielectric stacks (for 100 and 200 layers) would exhibit a small imaginary part of the index over the wavelength range for negative refraction. This established a new approach for thick, low-loss metamaterials at infrared and optical frequencies. This theoretically suggested multilayer NIM design [63] was recently modified, and corresponding structures with up to three functional layers (seven actual layers) were fabricated by the Karlsruhe group [64]. The silver-based samples were fabricated by standard electron-beam lithography, metal and dielectric depositions and a lift-off procedure with processing steps similar to those for creating a single NIM layer [21,22] (Fig. 5). The measured performance of the fabricated NIMs was found to be close to theory, and the retrieved optical parameters ($n' = -1$ at 1.4 μm) did not change much with the number of functional layers, as expected for an ideal metamaterial.

While the realization of such a three-functional-layer NIM can be seen as a first step towards three-dimensional photonic metamaterials, the fabrication of thicker NIM slabs using this approach will be increasingly difficult. This issue is related to the fact that in a standard deposition, lift-off procedure, the total thickness of the deposited layers is limited by the thickness of the patterned e-beam resist. For a successful lift-off procedure, the total deposited thickness should normally be at least 15–20% less than the thickness of the resist (Fig. 6). This value is usually not more than a couple 100 nm (for e-beam writing structures with sub-100-nm features). As mentioned above (2D fabrication via EBL), an aspect ratio exceeding unity poses significant fabrication challenges. Moreover, this fabrication procedure results in non-rectangular sidewalls, typically with an angle of about 10° with respect to the substrate normal on all

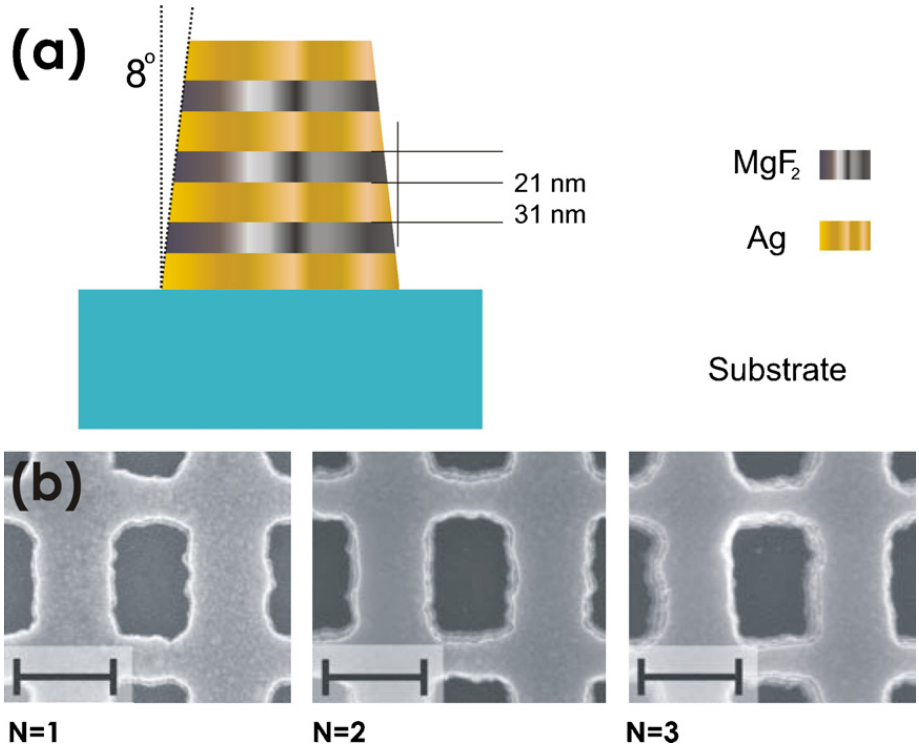

Fig. 5. (a) Schematic (side view) of the metamaterial layers under investigation together with (b) electron micrographs of fabricated structures with *N*-functional layers (400-nm scale bar) [64].

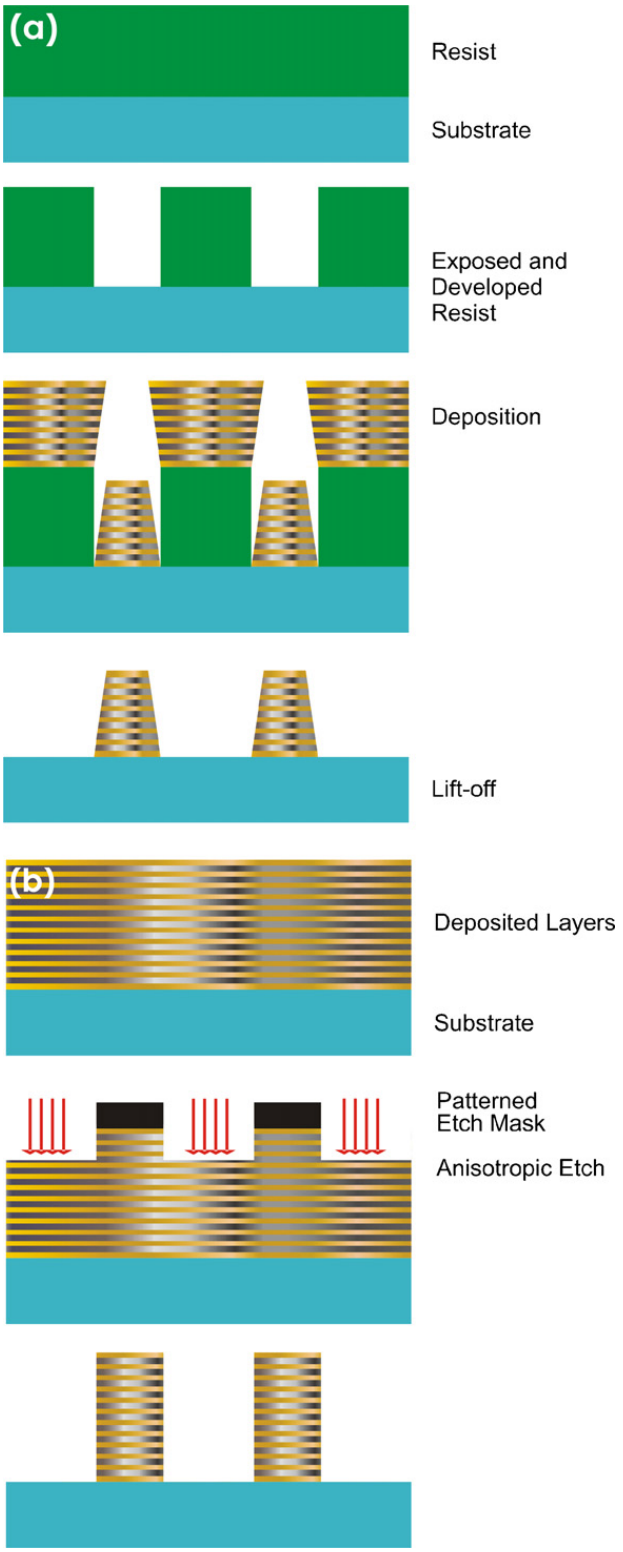

Fig. 6. Schematic of two possible ways of making multiple metal–dielectric layers: (a) the standard deposition—lift-off procedure [64] that provides trapezoidal final structures and has a total deposited thickness limitation (it has to be at least 15–20% less than the thickness of the resist for a successful lift-off process) together with (b) the proposed etch-based procedure where a thick planar stack of metal–dielectric layers is deep etched to create a 3D metamaterial slab.

sides [19,64] (Fig. 6). Obviously, this effect becomes particularly large for thick, multilayer structures.

To overcome problems connected to the lift-off procedure and non-rectangular sidewalls, and to create thicker NIM stacks, an alternative approach was suggested by a research group in Stuttgart [65]. In their approach, a stack of 3D optical NIMs, was realized through a layer-by-layer technique similar to that developed for 3D photonic crystal fabrication [66]. In the experiment, a four-layer split-ring resonator structure was fabricated. A single SRR layer was fabricated by simple metal evaporation, electron beam exposure, development and ion-beam etching of the metal. Since the non-planar surface of the single SRR layer does not allow simple stacking by a serial layer-by-layer process, the surfaces of the SRR layers were flattened by applying a planarization procedure with dielectric spacers (the roughness of the planarized surface was controlled within 5 nm). The procedures of single-layer fabrication, planarization and lateral alignment of subsequent layers were repeated several times yielding the four-layer SRR sample [65] (Fig. 7).

Even though the developed layer-by-layer technique can be seen as a general method for the manufacture 3D optical NIMs, such a step-by-step method requires additional process development (like planarization techniques) and careful lateral alignment of different layers that are crucial for successful stacking. Together with EBL fabrication of a single layer, alignment procedures lead to increased fabrication time. Thus, this approach is still too costly and has a low throughput for creating large-scale 3D metamaterial slabs for possible applications.

Another way to truly create a 3D, multiple-layer NIM could be a process based on deep, anisotropic etching. In such an approach, one would first fabricate planar, alternating metal and dielectric layers of any desired thickness, after which a deep etch would be performed using an etch mask pre-patterned to any required design by lithographic means (Fig. 6). However, this approach requires both heavy material and process developments, including the careful choice of etch-resistant mask materials and anisotropic etch optimization so that both the metal and dielectric layers can be etched.

4.2. Two-photon-photopolymerization (TPP) technology

The two-photon photopolymerization technique has been used extensively in the past few years to realize 3D patterning [67,68]. TPP involves the polymerization of a material via a nonlinear, multiphoton process that

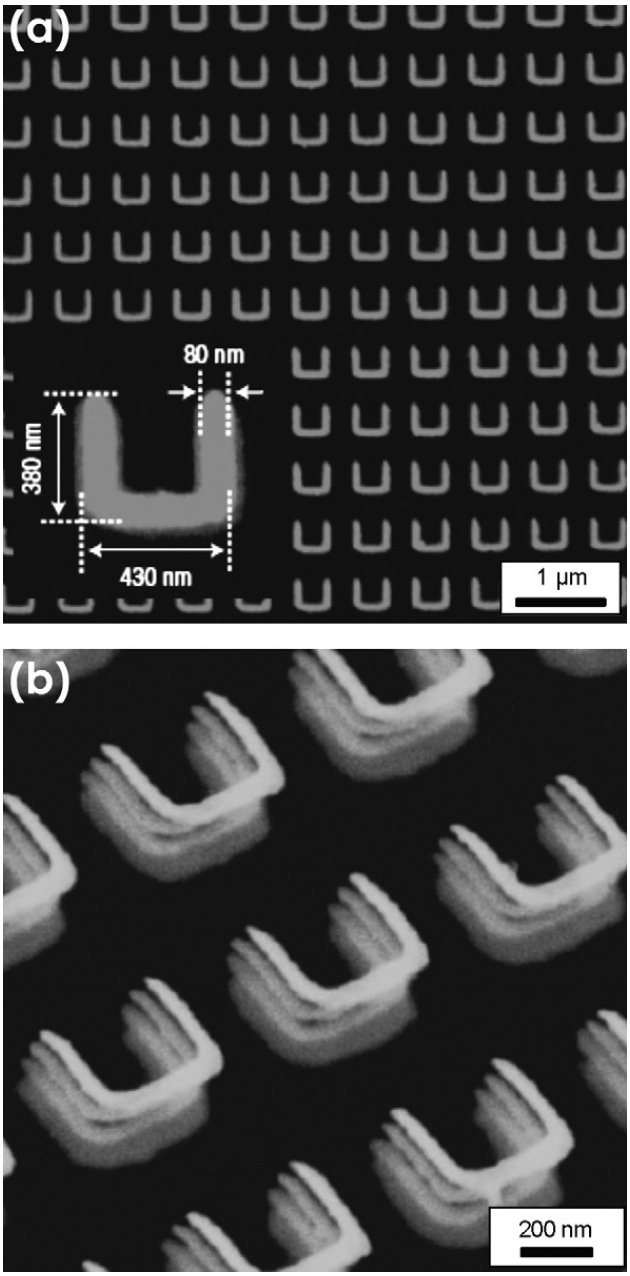

Fig. 7. Field-emission scanning electron microscopy images of the four-layer SRR structure: (a) normal view and (b) enlarged oblique view [65].

only occurs at the focal point of a tightly focused laser beam, thereby providing 3D control over the location of polymerization. TPP enables the fabrication of complex objects with ‘diffraction resolutions [69] since the absorption of light in the material occurs only at the focal region of the laser beam.

While most studies on TPP have focused on the realization of polymeric structures [68–70], this technique was recently studied for the fabrication of metallic 3D patterns [71,72]. Recent realizations of 3D, periodic, metallic structures over large areas was achieved through a TPP technique combined with a microlens array [73]. This technique is a step forward from standard, single-beam laser writing into a polymer matrix, which is time-consuming and thus unlikely to be adopted for large-scale fabrication. The proposed method, however, enabled the simultaneously writing of more than 700 polymer structures that were uniform in size. The metallization of the structures was then achieved through the deposition of thin films composed of small silver particles by means of electroless plating (Fig. 8). A hydrophobic coating on the substrate prevented silver deposition in unwanted areas and allowed the formation of a large number of isolated and highly conducting objects. This of metallization is flexible in that it can produce either polymer structures covered with metal or numerous isolated, insulating polymer objects spread over a metallic film, depending on the resin properties and treatment procedures [71,73]. TPP-based laser writing is now considered to be one of the most promising methods for future manufacturing of large-area, true 3D metamaterials. Offering intrinsic 3D parallel processing capability with acceptable resolution (100 nm [69]), TPP can be successfully combined with selective metal deposition by electroless plating [71–73].

While TPP enables arbitrary sculpting below the micrometer scale, electroless plating can provide thin coatings of various metals. Going in this direction, process development and optimization is required in order to include metal–dielectric layers into a polymer template made by TPP. In addition to electroless deposition, multimaterial deposition (including metal like silver) can be achieved via chemical vapor deposition (CVD) [74,75], which is a chemical process used to deposit high-purity materials. Both approaches need further advances and developments for creating thin, uniform and smooth layers of different materials on a TPP-fabricated polymer matrix.

4.3. Fabrication of complex 3D structures

Complex 3D metal–dielectric nanostructures can be fabricated today by several techniques. Considerable attention was recently attracted by two methods: direct electron-beam writing (EBW) [76] and focused-ion beam chemical vapor deposition (FIB-CVD) [77]. These methods offer 3D fabrication that is not possible using traditional layered optical and electron-beam lithographic techniques. The use of EBW was demonstrated for building structures of multiple layers with linewidth resolutions of 80–100 nm using an electron beam to cause direct sintering of 2–10 nm nanoparti-

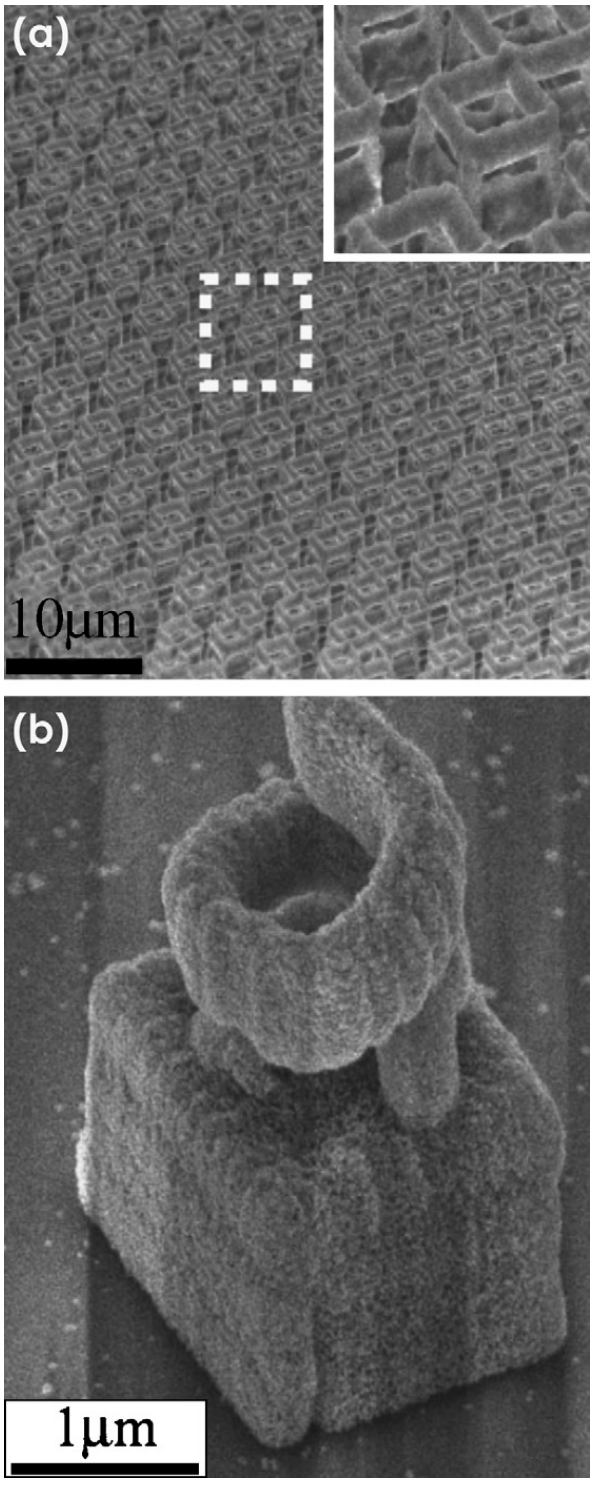

Fig. 8. Scanning electron microscope images of (a) self-standing empty cubic structures (height ~4.6 μm) connected in pairs and (b) a silver-coated polymer structure composed of a cube (2 μm in size) holding up a spring (inner diameter 700 nm) [71]. The structures are made by a two-photon induced photopolymerization technique combined with electroless plating [71–73]. Reused with permission from Florian Formanek, Nobuyuki Takeyasu, Takuo Tanaka, Kenta Chiyoda, Atsushi Ishikawa, and Satoshi Kawata, Applied Physics Letters 88 (2006) 083110. Copyright 2006, American Institute of Physics.

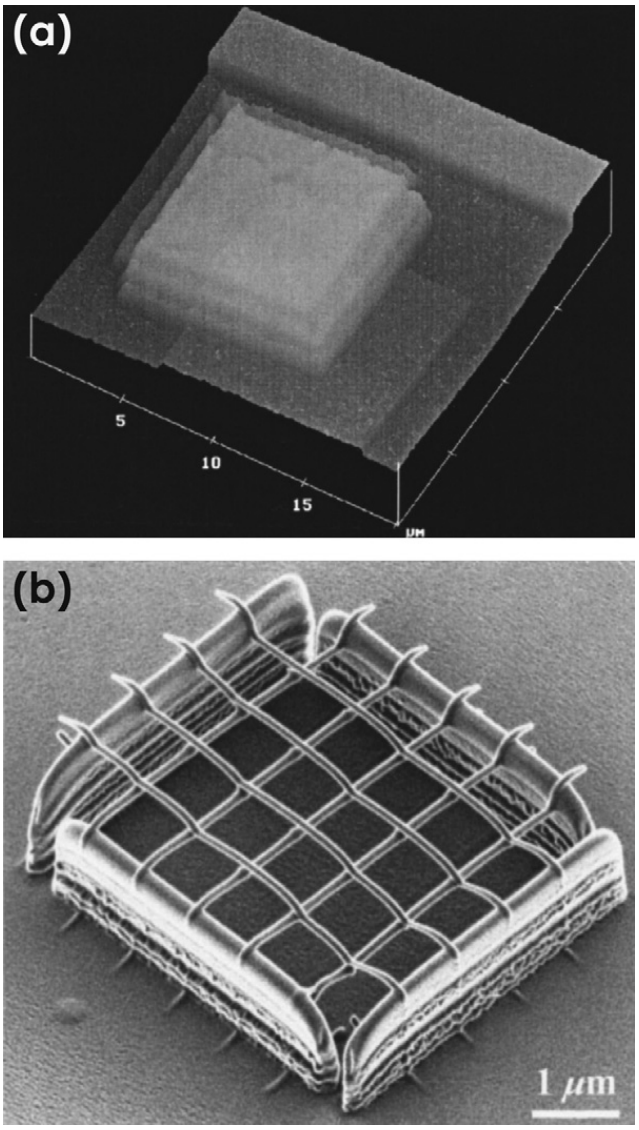

Fig. 9. Towards complex 3D structures: (a) atomic force microscope image of a multilayer (Ag–Au–Ag) structure prepared by electron-beam exposure of solutions of thiol-capped metal nanoparticles (electron-beam stereolithography process) [76] and (b) scanning ion microscope image of a crossbar circuit structure fabricated by using focused-ion beam chemical vapor deposition [77] (conducting wires contain Ga and W). (a) has been reused with permission from Saul Griffith, Mark Mondol, David S. Kong, and Joseph M. Jacobson, Journal of Vacuum Science & Technology B 20 (2002) 2768. Copyright 2002, AVS The Science & Technology Society. (b) has been reused with permission from Takahiko Morita, Ken-ichiro Nakamatsu, Kazuhiro Kanda, Yuichi Haruyama, Kazushige Kondo, Takayuki Hoshino, Takashi Kaito, Jun-ichi Fujita, Toshinari Ichihashi, Masahiko Ishida, Yukinori Ochiai, Tsutomu Tajima, and Shinji Matsui, Journal of Vacuum Science & Technology B 22 (2004) 3137. Copyright 2004, AVS The Science & Technology Society.

cles [76], while various free-space Ga- and W-containing nanowirings were successfully fabricated by FIB-CVD also called 'free-space-nanowiring' fabrication technology [77] (Fig. 9).

In the EBW process [76], an additive-layer build technique for multiple-material functionality was developed. The processing steps involved spin-coated or drawn-down solutions of thiol-capped nanoparticles (either Ag or Au) onto silicon wafers, glass slides, or polyimide films. The resultant nanoparticle films were patterned by electron-beam and showed conductivity for the patterned metals within one order of magnitude of their bulk material properties. Multiple layer fabrication was successfully demonstrated by repeating the processing steps for subsequent layers spun over previously patterned features. Further material and process optimization (for example, to allow combinations of multiple materials) may lead to EBW adoption for test fabrications of complex metamaterials.

While these and similar [78] nanofabrication techniques offer unique possibilities for making very complex 3D structures, they all suffer from severe material limitations in terms of what materials can be patterned/deposited. Moreover, such methods are complex and time-consuming. Thus they can only be used for making first prototypes or single structures for proof-of-principle studies.

Complex 3D metallic structures can also be fabricated using layer-by-layer repetition of standard planar processes. Recently, 3D tungsten photonic crystals were fabricated using a modified planar silicon MEMS process developed at Sandia National Labs [79]. In this approach, a patterned silicon dioxide mould is filled with a 500-nm-thick tungsten film and planarized using a chemical mechanical polishing process. This process is repeated several times, and at the end of the process the silicon dioxide is released from the substrate, leaving a freely standing thin patterned tungsten film. This method allows the patterning of multilayered (up to 60) samples of large area ($\sim$cm^2).

Another process for the parallel fabrication of microcomponents is the LIGA microfabrication technique. LIGA is an acronym referring to the main steps of the process, i.e., deep X-ray lithography (DXRL), electroforming, and plastic moulding. These three steps make it possible to mass-produce microcomponents at a low cost. Recently, the LIGA method was used by Sandia National Labs to fabricate 3D photonic lattices [79]. In this approach, the 3D lattice is patterned using deep X-ray lithography to create a series of intersecting channels in a polymer. This technique makes it possible to create large area moulds that can be filled with gold by electroplating techniques. Large-scale woodpile structures with gold as the matrix material were recently demonstrated [79].

4.4. 3D structures by nanoimprint

As an ultra-high resolution patterning technique simultaneously offering sub-50-nm resolution and sub-10-nm layer alignment capability, NIL can be used in multilayer processes for creating 3D structures. NIL has the potential for very large-scale and inexpensive manufacture of structures via multilayer lithography, alignment, and plating techniques. For example, 3D cubic arrays of gold cubes separated by a polymer were recently fabricated [79]; such arrays can act as photonic crystals. This rapid-prototyping contact lithography approach provides a platform for investigating new structures, materials, and multilayer alignment techniques that are critical for device designs at optical operational wavelengths.

Three-dimensional polymer structures can also be realized by a newly developed nanofabrication technique, namely reverse-contact UV nanoimprint lithography [80], which is a combination of NIL and contact printing lithography. In this process, a lift-off resist and a UV cross-linkable polymer are spin-coated successively onto a patterned UV mask-mould. These thin polymer films are then transferred from the mould to the substrate by contact at a suitable temperature and pressure. The whole assembly is then exposed to UV light. After separation of the mould and the substrate, the unexposed polymer areas are dissolved in a developer solution leaving behind the negative features of the original stamp. This method delivers resist pattern transfer without a residual layer, thereby rending unnecessary the etching steps typically needed in the imprint lithography techniques for three-dimensional patterning. This method is reproducible over millimeter-scale surface areas and has already provided encouraging results for fabricating 3D woodpile-like structures for polymer photonic devices [80]. Combined with multimaterial deposition similar to the TPP case, this approach might also be adapted for future NIM fabrication.

4.5. Self-assembly

In searching for ways of creating a true 3D metamaterial, one should also draw attention to the recent advances in the fabrication of 3D photonic crystals (PCs) [81,82], artificially designed material systems in which their optical properties largely derive from the system structure rather than from the material itself. Similar to the case of metamaterials, PC fabrication requires different techniques for creating periodic structures built of materials with alternating refractive indices. Recent reviews on the fabrication of 3D photonic crystals tend

towards synthesis methods based on *self-assembly* to realize such materials in the optical range. In the self-assembly approach, *opals* have received a strong backing from their ability to be used as scaffoldings for further templating of other materials [83]. In the fabrication procedure, the formation of the templates (opals) is followed by the subsequent synthesis of guest materials such as semiconductors, metals and/or insulators and, if desired, additional 2D patterning for the design of new structures. Accurate amounts of silicon, germanium, silica, etc., can be grown in the interior the opal structures by CVD, allowing the fabrication of multilayer systems of different materials [83]. The use of opals to pattern the growth of other materials (including metals) and subsequent vertical and lateral engineering of the fabricated structures have also been demonstrated [83]. This method, though not directly applicable to metamaterial fabrication at the moment, comprises fabrication steps that are of vital importance for future 3D metamaterials, namely pre-patterned, controllable growth of different materials including metals.

For the realization of 3D, metallic, periodic structures on a large scale, the self-organization of metal-coated colloid particles was successfully employed [84]. However, similar to opal structures, this method is difficult to employ for metamaterial fabrication requiring the creation of specially designed shapes.

Recently, another self-assembly approach was suggested for the realization of 3D NIMs for the microwave and optical frequencies [85]. By using a metal–dielectric, stress-actuated, self-assembly method, periodic arrays of metal flap SRRs and hinges were fabricated by lithographic patterning combined with metal deposition, lift-off and etching procedures. This approach offers large-scale fabrication and can in principle be scalable from microwave (100 GHz) to optical frequencies (300 THz). However, for creating optical NIMs, the careful choice of materials as well as the close control of geometrical parameters and release etching chemistry is required. Moreover, combined with the fabrication challenges, moving to the optical range will bring up the limit of size scaling in SRR functionality [18].

5. Thin metal film deposition

Aside from the requirements of nanometer-scale resolution and high throughput, highly controllable thin-film deposition methods are needed for the realization of good performance (low loss) NIMs. Whatever approach is chosen as a manufacturing method for the next generation of optical NIMs, the possibility of creating thin metal and dielectric films with reduced surface roughness is vital. High *roughness* of the metal film is the main limit to obtaining lower-loss metamaterials since it leads to increased scattering losses in the system and can annihilate the negative-index effect [15].

Depending on the chosen approach, different deposition techniques have to be studied and optimized. For example, in the standard lithography – deposition – lift-off procedure [15,19,22–24], the roughness of the e-beam-evaporated metal films can be reduced by the proper choice of the deposition conditions [15]. The quality of the deposited metal film depends also on the quality of the dielectric spacer layer. Especially in the case of an unstable metal like silver [86–88], the roughness of the initial dielectric structure is very important since clusters and lumps on a dielectric surface can, for example, work as seeds for the induced silver restructuring. The conventional way to improve the quality of the metal film is to use a *lower deposition rate* and a dielectric material with *stronger adhesion* and better surface quality. For example, the decrease of the deposition rate from 2 Å/s to 0.5 Å/s resulted in improved surface roughness and, hence, better optical performance of a recent magnetic metamaterial [15]. However, the decrease in the deposition rate leads to heating of the structure during deposition that makes the following lift-of process more difficult. Thus, higher complexity, multi-step deposition procedures were required [15].

In the case of silver, which is the most-used metal for optical NIMs [15,22–24] due to its optical properties, air exposure is also a problem since silver degrades under ambient conditions. The deposition of a dielectric layer on top of the structure [15,24] can help to prevent silver deterioration. In order to improve the structure further, *annealing* can also be applied [86].

When considering approaches that are feasible for future 3D NIM fabrication, specifically direct laser writing based on TPP or 3D interference lithography yielding complex polymer structures, deposition methods different from standard deposition and sputtering techniques must be developed. Here, metal deposition by *electroless plating* seems to be one of the possible directions. As mentioned above, this approach was recently applied to selectively deposit metal on a polymer structure [71–73]. Electroless plating has also been shown to be a promising way of achieving controllable deposition of thin metal films with low roughness (average roughness below 2 nm) [89]. In light of future NIM manufacturing where controllable coating of complex 3D structures is required, alternative metal deposition techniques like chemical vapor deposition [74], polymer-assisted [90] and nanoparticles-assisted [91] deposition have to be explored as well.

6. Discussion and outlook

The fabrication of optical negative-refractive-index metamaterials is quite challenging, due to the requirements of 100- and sub-100-nm feature sizes of the "meta-atoms" and small periodicities on the order of 300 nm or less. Due to the high-resolution requirement, electron-beam lithography is still the first choice for fabricating small-area metamaterials ($\sim$100 μm $\times$ 100 μm) [19,22–24]. Writing larger areas requires long e-beam writing times and hence, boosts the operation cost. Thus, this approach is only suitable for proof-of-principle studies. Similar to EBL, other serial processes, for example the focused-ion beam milling technique [17], are not considered to be feasible for the large-scale metamaterial fabrication required by applications.

One approach to manufacturing high-quality NIMs on a large scale ($\sim$cm^2 areas) is provided by interference lithography [20,53,55]. To increase the resolution, IL can be combined with self-assembly techniques [52]. Moreover, this technique could also be applied to the fabrication of future 3D metamaterials by piling 2D layers into a 3D structure. This step of stacking individual 2D layers made by IL has not been accomplished yet.

Another promising approach to create large-scale, high-quality metamaterials is nanoimprint lithography [58,92]. NIL offers nanoscale resolution; it is a parallel process with high throughput and, hence, a good candidate for NIM fabrication. Since NIL requires a stamp made by other nanofabrication techniques (like EBL) it is ideal for parallel production of already optimized metamaterials, when the preliminary test structures were patterned via EBL. Thus, NIL can be seen as a large-scale, low-cost process of making EBL-written structures that offers solutions to the intrinsic EBL drawbacks.

The first steps towards the realization of a 3D NIM were made by creating a multilayer structures (instead of a single functional layer) [64] and by utilizing a layer-by-layer technique [65]. Both approaches of making stacked metamaterials still have limitations (like challenging lift-off procedure in the first method and alignment requirements in the second). Another possible direction of making multiple-layer NIMs could be to consider deep anisotropic etching of a pre-fabricated multilayer stack. However, this approach has not been pursued yet due to the challenges connected to the dry etch of metal–dielectric stacks.

While complex 3D nanostructures can be fabricated today by several techniques (for example, direct electron-beam writing [76] and focused-ion beam chemical vapor deposition [77]), these methods are too complex and time-consuming to be adapted for large-scale NIM fabrication.

A fabrication method that is now considered to be one of the most promising approaches for future manufacturing of large-area, true 3D metamaterials is based on two-photon photopolymerization techniques [71,72]. While offering sub-diffraction resolution (down to 100 nm) [69] due to a nonlinear multiphoton process, this technique possesses intrinsic 3D processing capability. In addition to direct single-beam laser writing of complex structures into a polymer matrix, large-scale 3D polymer structures for future real-life applications can be realized via a 3D, multiple-beam TPP technique [73]. When combined with selective metal deposition by electroless plating [71–73] or via chemical vapor deposition, TPP can enable arbitrary 100-nm scale sculpturing of metal–dielectric structures. However, this approach needs further advances and developments for creating thin, uniform and smooth layers of different materials on a TPP-fabricated polymer matrix.

Three-dimensional, multilayered, polymer and metallic structures can also be realized by nanoimprint lithography [79,80]. This method offers high reproducibility over large areas (millimeter scale) and has been used for fabricating 3D cubic arrays of gold cubes and 3D woodpile-like polymer structures for photonic crystal-based devices [79,80]. Combined with multimaterial deposition, these approaches might also be adapted for future NIM fabrication.

To reach real NIM applications, several tasks have to be fulfilled: loss reduction, large-scale 3D fabrication and new isotropic designs. Careful material choice (for example, new crystalline metals with lower absorption instead of traditional silver and gold) and process optimization (reduced roughness and high uniformity of the materials) can help on the way to creating low-loss optical NIMs. Another possibility is to introduce a gain material into the NIM, thus compensating for losses. Even though it is still a long way to truly three-dimensional, isotropic, negative-index metamaterials at optical frequencies, several fabrication approaches do seem to be feasible. With emerging techniques such as nanoimprint, contact lithography, direct laser writing and possibly new types of self-assembly, it seems likely that truly 3D metamaterials with meta-atom sizes much smaller than the wavelength can be created. In the next generation of optical NIMs, for any chosen manufacturing approach, the careful choice of materials and process optimization will be required in order to obtain high-quality structures. Thus, a discussion of future fabrication tool selection needs to be based on careful considerations of the structural quality achiev-

able with the suggested method and the associated cost.

Acknowledgements

The authors would like to acknowledge support from the Danish Research Council for Technology and Production Sciences (FTP) grant no. 274-07-0057 (AB), ARO-MURI Award 50432-PH-MUR and NSF-PREM DMR-0611430 (VS).

References

[1] V.G. Veselago, The electrodynamics of substances with simultaneously negative values of ε and μ, Sov. Phys. Usp. 10 (1968) 509.
[2] V.G. Veselago, L. Braginsky, V. Shklover, Ch. Hafner, Negative refractive index materials, J. Comput. Theor. Nanosci. 3 (2006) 189.
[3] J.B. Pendry, Negative refraction, Contemp. Phys. 45 (2004) 191.
[4] V.G. Veselago, E. Narimanov, The left hand of brightness: past, present and future of negative index materials, Nat. Mater. 5 (2006) 759.
[5] V.M. Shalaev, Optical negative-index metamaterials, Nat. Photon. 1 (2007) 41.
[6] C.M. Soukoulis, M. Kafesaki, E.N. Economou, Negative-index materials: new frontier in optics, Adv. Mater. 18 (2006)1941.
[7] J.B. Pendry, Negative refraction makes a perfect lens, Phys. Rev. Lett. 85 (2000) 3966.
[8] J.B. Pendry, A.J. Holden, D.J. Robbins, W.J. Stewart, Magnetism from conductors and enhanced nonlinear phenomena, IEEE Trans. Microw. Theory Techn. 47 (1999) 2075.
[9] R.A. Shelby, D.R. Smith, S. Schultz, Experimental verification of a negative index of refraction, Science 292 (2001) 77.
[10] T.J. Yen, W.J. Padilla, N. Fang, D.C. Vier, D.R. Smith, J.B. Pendry, D.N. Basov, X. Zhang, Terahertz magnetic response from artificial materials, Science 303 (2004) 1494.
[11] S. Zhang, W. Fan, B.K. Minhas, A. Frauenglass, K.J. Malloy, S.R.J. Brueck, Midinfrared resonant magnetic nanostructures exhibiting a negative permeability, Phys. Rev. Lett. 94 (2005) 037402–37404.
[12] N. Katsarakis, G. Konstantinidis, A. Kostopoulos, R.S. Penciu, T.F. Gundogdu, M. Kafesaki, E.N. Economou, T. Koschny, C.M. Soukoulis, Magnetic response of split-ring resonators in the far-infrared frequency regime, Opt. Lett. 30 (2005) 1348.
[13] S. Linden, C. Enkrich, M. Wegener, J. Zhou, T. Koschny, C.M. Soukoulis, Magnetic response of metamaterials at 100-THz, Science 306 (2004) 1351.
[14] C. Enkrich, M. Wegener, S. Linden, S. Burger, L. Zschiedrich, F. Schmidt, J.F. Zhou, T. Koschny, C.M. Soukoulis, Magnetic metamaterials at telecommunication and visible frequencies, Phys. Rev. Lett. 95 (2005) 203901–203904.
[15] H.K. Yuan, U.K. Chettiar, W. Cai, A.V. Kildishev, A. Boltasseva, V.P. Drachev, V.M. Shalaev, A negative permeability material at red light, Opt. Express 15 (2007) 1076.
[16] W. Cai, U.K. Chettiar, H.K. Yuan, V.C. De Silva, A.V. Kildishev, V.P. Drachev, V.M. Shalaev, Metamagnetics with rainbow colors, Opt. Express 15 (2007) 3341.
[17] C. Enkrich, F. Perez-Williard, D. Gerthsen, J. Zhou, T. Koschny, C.M. Soukoulis, M. Wegener, S. Linden, Focused-ion-beam nanofabrication of near-infrared magnetic metamaterials, Adv. Mater. 17 (2005) 2547.
[18] W.M. Klein, C. Enkrich, M. Wegener, C.M. Soukoulis, S. Linden, Single-slit split-ring resonators at optical frequencies: limits of size scaling, Opt. Lett. 31 (2006) 1259.
[19] V.M. Shalaev, W. Cai, U.K. Chettiar, H.K. Yuan, A.K. Sarychev, V.P. Drachev, A.V. Kildishev, Negative index of refraction in optical metamaterials, Opt. Lett. 30 (2006) 3356.
[20] S. Zhang, W. Fan, N.C. Panoiu, K.J. Malloy, R.M. Osgood, S.R.J. Brueck, Experimental demonstration of near-infrared negative-index metamaterials, Phys. Rev. Lett. 95 (2005) 137404.
[21] G. Dolling, C. Enkrich, M. Wegener, C.M. Soukoulis, S. Linden, Simultaneous negative phase and group velocity of light in a metamaterial, Science 312 (2006) 892.
[22] G. Dolling, C. Enkrich, M. Wegener, C.M. Soukoulis, S. Linden, Low-loss negative-index metamaterial at telecommunication wavelengths, Opt. Lett. 31 (2006) 1800.
[23] G. Dolling, M. Wegener, C.M. Soukoulis, S. Linden, Negative-index metamaterial at 780 nm wavelength, Opt. Lett. 32 (2007) 53.
[24] U.K. Chettiar, A.V. Kildishev, H.K. Yuan, W. Cai, S. Xiao, V.P. Drachev, V.M. Shalaev, Dual-band negative index metamaterial: double negative at 813 nm and single negative at 772 nm, Opt. Lett. 32 (2007) 1671.
[25] S. Zhang, W. Fan, K.J. Malloy, S.R.J. Brueck, N.C. Panoiu, R.M. Osgood, Near-infrared double negative metamaterials, Opt. Express 13 (2005) 4922.
[26] T.A. Klar, A.V. Kildishev, V.P. Drachev, V.M. Shalaev, Negative-index metamaterials: going optical, IEEE J. Sel. Top. Quant. Electron. 12 (2006) 1106–1115.
[27] A.K. Popov, V.M. Shalaev, Compensating losses in negative-index metamaterials by optical parametric amplification, Opt. Lett. 31 (2006) 2169–2171.
[28] A.K. Popov, S.A. Myslivets, T.F. George, V.M. Shalaev, Four-wave mixing, quantum control and compensating losses in doped negative-index photonic metamaterials, Opt. Lett. 32 (2007) 3044–3046.
[29] V.M. Agranovich, Y.R. Shen, R.H. Baughman, A.A. Zakhidov, Linear and nonlinear wave propagation in negative refraction metamaterials, Phys. Rev. B 69 (2004) 165112.
[30] M. Lapine, M. Gorkunov, K.H. Ringhofer, Phys. Rev. E 67 (2003) 065601.
[31] M. Mattiucci, G. D'Aguanno, M.J. Bloemer, M. Scalora, Second harmonic generation from a positive-negative index material heterostructure, Phys. Rev. E 72 (2005) 066612.
[32] A.A. Zharov, I.V. Shadrivov, Y.S. Kivshar, Nonlinear properties of left-handed metamaterials, Phys. Rev. Lett 91 (2003) 037401.
[33] A.K. Popov, V.M. Shalaev, Negative-index metamaterials: second-harmonic generation. Manley-Rowe relations and parametric amplifications, Appl. Phys. B 84 (2006) 131.
[34] M.V. Gorkunov, I.V. Shadrivov, Y.S. Kivshar, Enhanced parametric processes in binary metamaterials, Appl. Phys. Lett. 88 (2006) 071912.
[35] N.M. Litchinitser, I.R. Gabitov, A.I. Maimistov, Optical bistability in a nonlinear optical coupler with a negative index channel, Phys. Rev. Lett. 99 (2007) 113902.
[36] M.W. Klein, M. Wegener, N. Feth, S. Linden, Experiments on second- and third-harmonic generation from magnetic metamaterials, Opt. Express 15 (2007) 5238–5247.

[37] M.W. Klein, C. Enkrich, M. Wegener, S. Linden, Second-harmonic generation from magnetic metamaterials, Science 313 (2006) 502–504.
[38] J.B. Pendry, D. Schurig, D.R. Smith, Controlling electromagnetic fields, Science 312 (2006) 1780–1782.
[39] U. Leonhardt, Optical conformal mapping, Science 312 (2006) 1777–1780.
[40] A.V. Kildishev, V.M. Shalaev, Engineering space for light via transformation optics, Opt. Lett. 33 (2008) 43–45.
[41] Z. Jacob, L.V. Alekseyev, E. Narimanov, Optical hyperlens: far-field imaging beyond the diffraction limit, Opt. Express 14 (2006) 8247–8256.
[42] A. Salandrino, N. Engheta, Far-field subdiffraction optical microscopy using metamaterials crystals: theory and simulations, Phys. Rev. B 74 (2006) 075103.
[43] Z. Liu, H. Lee, Y. Xiong, C. Sun, X. Zhang, Far-field optical hyperlens magnifying sub-diffraction-limited objects, Science 315 (2007) 1686.
[44] I.I. Smolyaninov, Y.-J. Hung, C.C. Davis, Magnifying superlens in the visible frequency range, Science 315 (2007) 1699–1701.
[45] E.E. Narimanov, V.M. Shalaev, Optics: beyond diffraction, Nature 447 (2007) 266–267.
[46] A.V. Kildishev, E.E. Narimanov, Impedance-matched hyperlens, Opt. Lett. 32 (2007) 3432–3434.
[47] D. Schurig, J.J. Mock, B.J. Justice, S.A. Cummer, J.B. Pendry, A.F. Starr, D.R. Smith, Metamaterial electromagnetic cloak at microwave frequencies, Science 314 (2006)977–980.
[48] W. Cai, U.K. Chettiar, A.V. Kildishev, V.M. Shalaev, Optical cloaking with metamaterials, Nat. Photon. 1 (2007) 224–227.
[49] W. Cai, U.K. Chettiar, A.V. Kildishev, G.W. Milton, V.M. Shalaev, Nonmagnetic cloak with minimized scattering, Appl. Phys. Lett. 91 (2007) 111105.
[50] W. Zhang, A. Potts, D.M. Bagnall, B.R. Davidson, Large area all-dielectric planar chiral metamaterials by electron beam lithography, J. Vac. Sci. Technol. B 24 (2006) 1455.
[51] W. Zhang, A. Potts, D.M. Bagnall, B.R. Davidson, High-resolution electron beam lithography for the fabrication of high-density dielectric metamaterials, Thin Solid Films 515 (2007) 3714.
[52] S.R.J. Brueck, Optical and interferometric lithography—nanotechnology enablers, Proc. IEEE 93 (2005) 1704.
[53] N. Feth, C. Enkrich, M. Wegener, S. Linden, Large-area magnetic metamaterials via compact interference lithography, Opt. Express 15 (2006) 501.
[54] S. Fan, S. Zhang, K.J. Malloy, S.R.J. Brueck, Large-area, infrared nanophotonic materials fabricated using interferometric lithography, J. Vac. Sci. Technol. B 23 (2005) 2700.
[55] S. Zhang, W. Fan, K.J. Malloy, S.R.J. Brueck, N.C. Panoiu, R.M. Osgood, Demonstration of metal–dielectric negative-index metamaterials with improved performance at optical frequencies, J. Opt. Soc. Am. B 23 (2006) 434.
[56] Z. Ku, S.R.J. Brueck, Comparison of negative refractive index materials with circular, elliptical and rectangular holes, Opt. Express 15 (2007) 4515.
[57] S.Y. Chou, P.R. Krauss, P.J. Renstrom, Nanoimprint lithography, J. Vac. Sci. Technol. B 14 (1996) 4129.
[58] W. Wu, E. Kim, E. Ponizovskaya, Z. Liu, Z. Yu, N. Fang, Y.R. Shen, A.M. Bratkovsky, W. Tong, C. Sun, X. Zhang, S.-Y. Wang, R.S. Williams, Optical metamaterials at near and mid-IR range fabricated by nanoimprint lithography, Appl. Phys. A 87 (2007) 147.
[59] W. Wu, Z. Yu, S.-Y. Wang, R.B. Williams, Y. Liu, C. Sun, X. Zhang, E. Kim, R. Shen, N. Fang, Midinfrared metamaterials fabricated by nanoimprint lithography, Appl. Phys. Lett. 90 (2007) 063107.
[60] Y. Chen, J. Tao, X. Zhao, Z. Cui, A.S. Schwanecke, N.I. Zheludev, Nanoimprint lithography for planar chiral photonic meta-materials, Microelectron. Eng. 78–79 (2005) 612.
[61] Y. Chen, Y. Zhou, G. Pan, E. Huq, Nanofabrication of SiC templates for direct hot embossing for metallic photonic structures and metamaterials, in: Micro- and Nano Engineering Conference Proceedings, MNE07, 2007, p. 592.
[62] S.W. Pang, T. Tamamura, M. Nakao, A. Ozawa, H. Masuda, Direct nano-printing on Al substrate using a SiC mold, J. Vac. Sci. Technol. B 16 (1998) 1145.
[63] S. Zhang, W. Fan, N.C. Panoiu, K.J. Malloy, R.M. Osgood, S.R.J. Brueck, Optical negative-index bulk metamaterials consisting of 2D perforated metal–dielectric stacks, Opt. Express 14 (2006) 6778.
[64] G. Dolling, M. Wegener, S. Linden, Realization of a three-functional-layer negative-index photonic metamaterial, Opt. Lett. 32 (2007) 551.
[65] N. Liu, H. Guo, L. Fu, S. Kaiser, H. Schweizer, H. Giessen, Three-dimensional photonic metamaterials at optical frequencies, Nat. Mater. 7 (2007) 31–37.
[66] S. Subramania, S.Y. Lin, Fabrication of three-dimensional photonic crystal with alignment based on electron beam lithography, Appl. Phys. Lett. 85 (2004) 5037.
[67] S. Maruo, O. Nakamura, S. Kawata, Three-dimensional microfabrication with two-photon-absorbed photopolymerization, Opt. Lett. 22 (1997) 132.
[68] S. Kawata, H.-B. Sun, T. Tanaka, K. Takada, Finer features for functional microdevices, Nature 412 (2001) 697.
[69] K. Takada, H.-B. Sun, S. Kawata, Improved spatial resolution and surface roughness in photopolymerization-based laser nanowriting, Appl. Phys. Lett. 86 (2005) 071122–71123.
[70] S. Passinger, S.M. Saifullah, C. Reinhardt, R.V. Subramanian, B. Chichkov, M.E. Welland, Direct 3D patterning of TiO_2 using femtosecond laser pulses, Adv. Mater. 19 (2007) 1218.
[71] F. Formanek, N. Takeyasu, K. Tanaka, K. Chiyoda, T. Ishihara, S. Kawata, Selective electroless plating to fabricate complex three-dimensional metallic micro/nanostructures, Appl. Phys. Lett. 88 (2006) 083110.
[72] N. Takeyasu, T. Tanaka, S. Kawata, Fabrication of 3D metal/polymer fine structures for 3D plasmonic metamaterials, in: Photonic Metamaterials: From Random to Periodic, OSA Technical Digest (CD), Optical Society of America, 2007, paper WD3.
[73] F. Formanek, N. Takeyasu, T. Tanaka, K. Chiyoda, A. Ishikawa, S. Kawata, Three-dimensional fabrication of metallic nanostructures over large areas by two-photon polymerization, Opt. Express 14 (2006) 800.
[74] Y. Chi, E. Lay, T.-Y. Chou, H.-Y. Song, A.J. Carty, Deposition of silver thin films using the pyrazolate complex $[Ag(3,5\text{-}(CF_3)_2C_3HN_2)]_3$, Chem. Vapor Depos. 11 (2007) 206.
[75] M. Wegener, Nature Materials (2008) in press.
[76] S. Griffith, M. Mondol, D.S. Kong, J.M. Jacobson, Nanostructure fabrication by direct electron-beam writing of nanoparticles, J. Vac. Sci. Technol. B 20 (2002) 2768.
[77] T. Morita, K. Nakamatsu, K. Kanda, Y. Haruyama, K. Kondo, T. Kaito, J. Fujita, T. Ichihashi, M. Ishida, Y. Ochiai, T. Tajima, S. Matsui, Nanomechanical switch fabrication by focused-ion-beam chemical vapor deposition, J. Vac. Sci. Technol. B 22 (2004) 3137.

[78] P. Hoffmann, Comparison of fabrication methods of sub-100 nm nano-optical structures and devices, Proc. SPIE 5925 (2005) 06–14.
[79] F.B. McCormick, J.C. Verley, A.R. Ellis, I. El-kady, D.W. Peters, M. Watts, W.C. Sweatt, J.J. Hudgens, J.G. Fleming, S. Mani, M.R. Tuck, J.D. Williams, C.L. Arrington, S.H. Kravitz, C. Schmidt, G. Subramania, Fabrication and characterization of large-area 3D photonic crystals, Aerospace Conf. IEEE (2006) 1.
[80] N. Kehagias, V. Reboud, G. Chansin, M. Zelsmann, C. Jeppesen, C. Schuster, M. Kubenz, F. Reuther, G. Gruetzner, C.M. Sotomayor Torres, Reverse-contact UV nanoimprint lithography for multilayered structure fabrication, Nanotechnology 18 (2007) 175303–175304.
[81] E. Yablonovitch, Photonic bang-gap structures, J. Opt. Soc. Am. B 10 (1993) 283.
[82] J.D. Joannopoulos, R.D. Meade, J.N. Winn, Photonic Crystals: Molding the Flow of Light, Princeton University Press, Princeton, USA, 1995.
[83] J.F. Galisteo, F. Garcýa-Santamarýa, D. Golmayo, B.H. Juarez, C. Lopez, E. Palacios, Self-assembly approach to optical metamaterials, J. Opt. A: Pure Appl. Opt. 7 (2005) S244–S254.
[84] Z. Chen, P. Zhan, Z. Wang, J. Zhang, W. Zhang, N. Ming, C.T. Chan, P. Sheng, Two- and three dimensional ordered structures of hollow silver spheres prepared by colloidal crystal templating, Adv. Mater. 16 (2004) 417.
[85] V.J. Logeeswaran, M. Saif Islam, M.-L. Chan, D.A. Horsley, W. Wu, S.-Y. Wang, Self-assembled microfabrication technology for 3D isotropic negative index materials, Proc. SPIE 6393 (2006) 639305–639310.
[86] H. Libardi, H.P. Grieneisen, Guided-mode resonance absorption in partly oxidized thin silver films, Thin Solid Films 333 (1998) 82.
[87] M. Del Re, R. Gouttebaron, J.P. Dauchot, P. Leclère, R. Lazzaroni, M. Wautelet, M. Hecq, Growth and morphology of magnetron sputter deposited silver films, Surf. Coat. Technol. 151–152 (2002) 86–90.
[88] V.P. Drachev, U.K. Chettiar, A.V. Kildishev, H.K. Yuan, W. Cai, V.M. Shalaev, The Ag dielectric function in plasmonic metamaterials, Opt. Express 16 (2008) 1186–1195.
[89] F. Jing, H. Tong, L. Kong, C. Wang, Electroless gold deposition on silicon(1 0 0) wafer based on a seed layer of silver, Appl. Phys. A 80 (2005) 597.
[90] Q.X. Jia, T.M. McCleskey, A.K. Burrell, Y. Lin, G.E. Collis, H. Wang, A.D.Q. Li, S.R. Foltyn, Polymer-assisted deposition of metal-oxide films, Nat. Mater. 3 (2004) 529.
[91] Y. Yan, S.-Z. Kang, J. Mu, Preparation of high quality Ag film from Ag nanoparticles, Appl. Surf. Sci. 253 (2007)4677.
[92] W. Wu, E. Kim, Y. Liu, E. Ponizovskaya, Z. Yu, A.M. Bratkovski, P. Chaturvedi, N.X. Fang, R. Shen, X. Zhang, Optical metamaterials fabricated by nano-imprint lithography, Proc. SPIE (2007) 6462.